

1 **Spatiotemporal Variability in Building Energy Use in New York City**

2 Y. Olivo ^{a,c}, A. Hamidi ^{b,c}, P. Ramamurthy ^{a,c,*}

3
4 ^aDepartment of Mechanical Engineering, CUNY City College of New York, New York, NY, USA

5 ^bDepartment of Civil Engineering, CUNY City College of New York, New York, NY, USA

6 ^cNOAA-CREST Center, CUNY City College of New York, New York, NY, USA

7 8 9 **Abstract**

10
11 Data on building energy use for large and dense cities is not yet available at adequate spatial and
12 temporal scales. The energy consumption from buildings significantly influences the local
13 climate and this impact is not adequately integrated into regional or local scale weather models.
14 The primary objective of his study is to understand and map building energy consumption and
15 quantify its impact on the urban environment; here, New York City (NYC) is used as a test case.
16 The project involved a detailed classification of buildings in NYC using a high-resolution
17 landuse/landcover dataset. The customized classification was then coupled with a single building
18 energy model (SBEM) to estimate the building energy use. The developed model matched the
19 annual energy use of NYC within 5% of the observed value. Coupled energy simulations were
20 then performed with the Weather Research and Forecasting (WRF) model. The results show that
21 heat released from building's heating and air conditioning system during extreme heat events can
22 be as high as 18% of the overall available energy. Finally, a comparison between the average
23 annual energy use, the urban heat island intensity (UHI) and the landcover/landuse fraction for
24 various parcels during extreme heat events indicated that neighborhoods surrounding the highly-
25 commercialized zones were disproportionately impacted by high UHI values. The increase was
26 related to advection of heat.

27 28 29 **1. Introduction**

30
31 Over the last three decades energy consumption and the corresponding greenhouse gas emissions
32 around the world have increased by approximately 49% and 43% respectively [1,2]. Energy
33 usage of developing countries is projected to rise 3.2% annually, eventually surpassing the
34 developed nations by 2020 [1]. The unabating consumption pattern will have adverse
35 consequences on both energy sustainability and improving climate resiliency [3,4]. One area of
36 importance is the building energy sector; currently, residential and commercial buildings in the
37 US account for 41% of the total energy consumed and 47% of the greenhouse gas emissions [5].
38 In China, 43% of the total energy consumption comes from building energy use [6]. In a dense
39 urban environment, such as New York City (NYC), buildings account for more than two-thirds
40 of total energy consumption [7]. The waste heat released from the buildings amplify the local air
41 temperature contributing to urban heat island effects and increases the probability of extreme
42 heat events in dense cities during the warm season [8,9]. Various studies have demonstrated the
43 feedback between electricity consumption and urban heat island intensity (UHI) [10,11]. Akbari
44 et al. (2009) showed that for every 1°C increase in air temperature, 2-4% more energy is required
45 to cool the indoor spaces for a large urban agglomeration. In addition to local impacts, urban
46 energy use also influences regional-scale water and energy cycles [12]. Currently various city,
47 state and federal administrations around the world have created various strategies to reduce the

48 overall energy consumption, restrict green house gas emissions, and moderate urban heat island
49 impacts [13-17]. However, without a clear understanding of the spatiotemporal correlations
50 between building energy use and its environmental impact, one cannot suitably address this
51 issue. The primary objective of this article is to understand the spatial and temporal pattern of
52 building energy use and its impact on the local environment in the densely populated New York
53 City. The research also aims to correlate the building energy use to urban landcover/landuse
54 pattern to identify land parcels for urban heat moderation strategies.
55

56 Recent studies have used both top-down and bottom-up approaches to predict energy
57 consumption in major cities with statistical analysis and estimations based on building functions
58 [7]. Sailor et al. (2004) used top-down approach using observations of electricity consumption
59 for different states in the U.S. to model temporal and spatial variability in energy consumption.
60 The model proved to be effective and found energy use to be highly dependent on population
61 density, which is highly variable and uncertain [18]. On a City scale, Howard et al. (2012)
62 developed a model to estimate the energy use for each tax lot in NYC. The model demonstrated
63 that energy consumption is highly dependent on the function of the building and not on the
64 building construction material [7]. Similar modeling approaches have also been used and proved
65 to be effective elsewhere outside of the United States. Momonoki et al. (2017) assessed the
66 effectiveness of bottom-up approach by evaluating energy use in residential sectors for Japan
67 creating a model based on building energy-use parameters (i.e. heating/cooling equipment,
68 insulation, weather). Simulation results were comparable to the statistical data for the residential
69 sector for the given modeling approach [19]. Menezes et al. (2014) studied the efficacy of
70 bottom-up approaches at a smaller scale, estimating the energy consumption of small power
71 equipment in office buildings in United Kingdom (UK). The model based on building function,
72 equipment used, and usage schedule demonstrated good correlation when compared to metered
73 data in the UK [20]. However, there are two main issues with inventory energy analysis: one, the
74 temporal resolution is highly restricted and two, there is a lack of data at fine spatial scales.
75

76 Another useful tool to conduct energy analysis is the single building energy model (SBEM). The
77 single building energy model created by the Department of Energy is a numerical scheme that
78 uses conductive and radiative heat transfer equations and numerous parametrizations that
79 account for occupancy, fenestration, heating and cooling efficiency to compute the energy load
80 for a given indoor and outdoor condition. The physical characteristics of the building, like roof
81 albedo, wall insulation and building material can all be independently parameterized. The model
82 is widely used by building operation managers and researchers to study and forecast energy use.
83 Heiple et al. (2008) simulated building energy consumption in Houston, Texas with SBEM and
84 found good agreement at individual building level [8]. Zerrouh et al. (2015) compared
85 electricity consumption from SBEM models to real data for individual buildings in Albuquerque,
86 New Mexico and concluded that SBEM can be used to model energy consumption for single
87 buildings [21]. Their results showed that the difference between SBEM and observations of
88 electricity consumption differed by approximately 4% on an annual basis. Lately, the single
89 building energy scheme is also used in regional climate models [21]. Ortiz et al. (2006) used the
90 coupled scheme to study the increase in energy load in NYC for heatwave episodes [22]. The
91 models are currently run at 1-3 km spatial resolution and hence the surface cover is parametrized
92 using bulk properties. As the spatial resolution of these models increase there is a greater need to

93 assess the scalability of the single building energy model to represent building envelope-
94 environment interactions.

95
96 Here we use the single building energy model integrated with a high-resolution building dataset
97 to study the spatial and temporal pattern of energy use in the densely populated New York City.
98 The analysis will include a detailed classification of buildings using local morphological
99 characteristics. Additionally, the energy use pattern will be coupled with a high-resolution
100 landcover dataset to identify land parcels that offer high potential for microclimate mitigation
101 strategies. The analysis will answer the following questions:

- 102
- 103 • What is the spatial and temporal variation in building energy consumption and heat
104 rejection in NYC?
- 105 • How is the energy consumption or demand partitioned between various commercial and
106 residential buildings?
- 107 • Can the single building energy model be scaled to represent energy use at neighborhood
108 and city scale?
- 109 • What neighborhoods/parcels within the city offer best potential for urban heat moderation
110 strategies?
- 111

112

113 **2. Methods and Validation**

114
115 Herein we detail the methods used in this investigation. The analysis presented here utilizes a
116 SBEM coupled to a localized building classification scheme to map the building energy use at
117 high spatial resolution. The SBEM output is validated using observations from a residential and a
118 commercial building. The energy model is then coupled to WRF to quantify the impact of
119 building energy use on the environment.

120 **2.1. Land Cover and Land Use Classification**

121
122 The study coupled publicly available data from the New York City Department of Planning
123 database also known as PLUTO (Public Land Use and Tax Lot database) with the single building
124 energy model [23]. The PLUTO database contains extensive information about buildings in
125 NYC that are preserved and updated by city organizations on a periodic basis. For each building,
126 the PLUTO database records its area, age, function, and other morphological parameters [23].
127 With this data, a detailed building classification scheme was implemented to represent the
128 complex local morphology. The buildings in the City were subdivided based on their primary
129 use: residential, commercial, or mixed. Each of these categories were then divided based on
130 physical characteristics such as building height (number of floors). Each residential, commercial,
131 and mixed building was divided into Low-rise (0-5 Floors), Mid-rise (6-20 Floors), and High-
132 rise (20+ Floors). The classifications were then modeled into a building energy model
133 independently. For each building model, a factor for electricity consumption per unit area was
134 derived. With this scaling factor, a bottom-up approach was implemented, which was shown to
135 be effective in other studies [8]. Utilizing the scaling factor obtained from simulations, we
136 computed the energy consumed and heat rejected utilizing the footprint of each building that fits
137 our classification scheme from the PLUTO database. The building energy model simulation was
138

139 carried out for year 2012. The classification scheme developed here is best suited for New York
140 City and will be different for other cities. Table 1 below illustrates the distribution of the
141 buildings in NYC. The categorization developed accounts for approximately 91 percent of the
142 total buildings in NYC (See Table 2). Buildings not included are: hospitals, parking lots, and
143 empty locations with an undefined building function.

144
145 NYC is primarily composed of residential buildings. Downtown and Midtown Manhattan,
146 specifically Times Square and Financial District areas, is dominated by commercial and mixed
147 building functions. In Brooklyn, the Williamsburg area and Flushing in Queens are populated by
148 commercial buildings. The commercial buildings in The Bronx are not concentrated in a specific
149 area, but are distributed around the borough (figure 2 illustrates the location of these
150 neighborhoods on the NYC map).

151
152 In addition to the PLUTO database that is used to classify the buildings, high resolution spatially
153 distributed land cover dataset, provided by NYC Department of Parks and Recreation [24] is
154 used here. The dataset, which has a spatial resolution of ~0.9 m, is derived using LiDAR
155 observations (from 2010) and 4-band orthoimagery, employing Object-Based Image Analysis
156 (OBIA) techniques. Around 23% of NYC land is covered by greens, ~31% by buildings and
157 ~17% by roads and pavements. In this analysis, we converted the data to the permeability
158 fraction according to the hydrological soil groups defined by the Department of Environment
159 Protection (DEP) guidelines [25]. For impervious surfaces, permeability fraction is assumed to
160 be 0 and for natural surfaces it varies between 0 - 100.

161

162

163 ***2.2. Single Building Energy Model (SBEM) and Model Validation***

164

165 The energy simulation was conducted using DOE-2 engine with eQuest as the front end [26].
166 The building energy model was validated with data from a commercial and a residential building
167 before upscaling using PLUTO. Monthly electricity consumption data from a two-story
168 residential building and a high-rise commercial building were obtained. The building
169 characteristics were modeled using data from the PLUTO database and the energy use was
170 simulated for a full year. The building properties were obtained from the DOE-2 in-built baseline
171 criteria for each of the respective building functions. Other factors that influence energy
172 consumption such as schedules, internal heat gains, as well as other building characteristics, were
173 determined based on the DOE-2 baseline model for respective building functions [26]. Nine
174 models were created in the SBEM; three for each of the respective building functions
175 (residential, commercial, and mixed) based on the building height (i.e. Low-rise, Mid-rise, High-
176 rise). The end-uses included in the calculation of energy consumption for each SBEM simulation
177 were also determined based on the building functions. The end-uses include: area lighting, task
178 lighting, miscellaneous equipment, ventilation fans, refrigeration, and space cooling [26]. As
179 with electricity consumption, heat rejected from the cooling system is an output generated from
180 the DOE-2 simulations. It is dependent on the HVAC system in use, which is different for
181 commercial and residential buildings. The single-zone DX coils cooling was used for residential
182 and mixed buildings and a chilled water loop cooling system was used for commercial buildings.
183 Table 3 shows the building properties used for the energy consumption simulations.

184

185 Fig. 1a illustrates the comparison between the modeled and observed electricity consumption for
186 a residential building. The results from the simulation follow the monthly trend for the entire
187 year reasonably well (See Fig. 1a). The coefficient of determination (R^2) is 0.74 and the RMSE
188 value is 1.68 kWh, which indicates a reasonably strong correlation between the simulated and
189 measured values. Similarly, Fig. 1b illustrates the comparison of electricity consumption
190 between high-rise model and the observations. The coefficient of determination (R^2) is 0.73 and
191 the RMSE value is 2.28 kWh. The trend for electricity consumption on a month by month basis
192 is very similar between the model and the real building. Given the local scale variability, related
193 to albedo, emissivity, insulation thickness, fenestration, occupancy and variability in forcing
194 data, the model performs reasonably well in estimating the monthly usage.

195
196

197 **2.3. Urban Climate Simulation**

198

199 The single building energy model simulation is a 1-way coupling and does not include the vital
200 feedbacks between energy use and its associated impacts on the environment. To enable this,
201 Weather Research and Forecast (WRF) model coupled with the building energy model and the
202 PLUTO database was used to simulate a 10-day period in 2012, between July 11 to July 21. It
203 should be noted that while the coupled simulations can quantify the impact of building energy
204 use on the environment, it is computationally expensive to perform lengthy simulations. Here,
205 we have focused on a 10-day period in mid-July that includes a heatwave scenario to capture the
206 impact of building energy use on the thermodynamic state of the urban environment. WRF is a
207 non-hydrostatic primitive Eq.-based model that has multiple options for parameterizations [27].
208 Fig. 3 shows the nested domains used for the simulation; 3 domains with grid resolutions $9 \times 3 \times$
209 1 km and 60 vertical grids centered on NYC were used. The North American Regional
210 Reanalysis (NARR) data at 6-hr intervals was used to drive the model and the North American
211 Land-use Category Dataset (NLCD) 2011 was used to determine the landuse type and the surface
212 properties. For New York City, the NLCD parameters were replaced by data from the PLUTO
213 database, which included building height, building area fraction and building surface ratio. The
214 simulation used the following physical parameterization schemes: (i) the rapid radiative transfer
215 model scheme for longwave radiation [28]; (ii) the Dudhia scheme for shortwave radiation [29];
216 (iii) the 2D Smagorinsky scheme for horizontal diffusion [30]; (iv) the mosaic Noah land surface
217 model for non-urban surfaces; (v) the Mellor–Yamada–Janjic PBL scheme [31] along with the
218 modified Zilitinkevich relationship for thermal roughness length parameterization [32]; (vi) the
219 BEP-BEM for urban parameterization. Cumulus parameterization schemes are not used in the
220 inner domain; however, they are enabled in the 2 outer domains. The model has been thoroughly
221 validated for the New York area using surface weather stations [22]

222

223

224 **3. Results and Discussion**

225

226 **3.1. Spatial & Temporal Variability**

227

228 The electricity consumption per unit area was obtained using the SBEM simulations, forced by
229 the DOE-2 built-in weather input file (Typical Meteorological Year version 2 (TMY2)). The
230 output was then integrated with our custom building classification scheme (detailed section 2.1)
231 and scaled up to city-level. Fig. 2 shows the spatial distribution of annual energy consumption.

232 The open spaces in the map indicate parks and airports. It is strikingly clear that the commercial
233 zones in downtown Manhattan consume the most electricity throughout the year (over 150
234 Megawatts-Hour). This area is occupied by densely packed commercial buildings. Other areas of
235 high electricity consumption include downtown Brooklyn near Williamsburg Bridge and Astoria
236 in Queens. These areas consume over 15 GWh of electricity on an annual basis. Areas
237 predominantly occupied by small residential houses had extremely low energy footprints
238 compared to the lower section of Manhattan. Overall, the commercial sector consumes
239 approximately ten times more electricity than the residential and mixed sectors for each of the
240 respective classifications, and much of this consumption is in Manhattan. Thus, in areas
241 dominated by commercial buildings, electricity consumption is higher than a predominantly
242 residential area during the daytime period. Fig. 3 illustrates the total electricity consumption for
243 each of the building classifications in this study for each of the respective boroughs in NYC.
244 Apart from Manhattan, in the outer boroughs the residential energy consumption is higher
245 compared to the commercial sector. In the Bronx and Queens residential high-rise buildings have
246 the highest consumption; whereas, in Brooklyn and Staten Island the consumption is much more
247 evenly distributed. In Manhattan, high-rise commercial and mixed buildings consume the most
248 electricity.

249
250 Heat rejected is an important parameter to study the anthropogenic impact on urban heat island
251 effects. We quantified the heat rejected from buildings using the same procedure used to
252 determine the electricity consumption. The heat rejected in NYC due to building energy
253 consumption follows the same spatial distribution as observed in Fig. 2. The categories
254 consuming the most electricity are also the categories responsible for rejecting the most heat into
255 the surroundings. Staten Island heat rejection is much lower than the other four boroughs
256 because it is comprised of primarily residential houses that are approximately 1 to 5 stories high.
257 The borough of Manhattan rejects the most heat out of all the boroughs, followed by Brooklyn,
258 Bronx, Queens, and Staten Island. In total 555 GWh was rejected during 2012 which averages
259 around 5.6 kWm^{-2} .

260
261 The Summer months had the highest electricity consumption; from June to August the total
262 energy use averaged to 3 Terawatt-hours for all three building types. From October to March it
263 averaged around 2 Terawatt-hours. The ratio of energy consumption between commercial and
264 residential buildings was 1:3, year around. Since most of the heat during the year is rejected over
265 the summer period, further analysis was conducted to understand how the heat rejected varies
266 depending on the daily conditions over an average summer day (Mean $23 \text{ }^\circ\text{C}$, Max $25 \text{ }^\circ\text{C}$) in
267 contrast to a heat wave day (Mean $31 \text{ }^\circ\text{C}$, Max $34 \text{ }^\circ\text{C}$). In NYC, any 3 consecutive days with a
268 daily maximum temperature exceeding $32 \text{ }^\circ\text{C}$ is considered a heat wave day [33]. The total heat
269 rejected over the average summer day was 4.47 Wm^{-2} while during a heat wave day the heat
270 rejected per unit of area was 9.33 Wm^{-2} . The difference between the average temperature
271 between the two days is $9 \text{ }^\circ\text{C}$. Highly commercialized zones such as Times Square rejected much
272 more heat than a residential area in Staten Island. For example, on a heat wave day, the highly
273 commercial zone of Times Square rejected twice as much heat, 16 Wm^{-2} . The heat rejected
274 from these zones could potentially impact areas that are downstream. NYC experiences strong
275 Southerly winds during daytime periods in the summer [34]. Hence much of the heat rejected in
276 the Downtown regions will impact the Upper Manhattan neighborhoods that have high
277 concentration of residents without air-conditioning.

278
279
280
281
282
283
284
285
286
287
288
289
290
291

Overall the results obtained provide a general picture of energy use pattern in NYC for the different building categories and neighborhoods. According to New York Independent Systems Operator (NYISO), the total electricity consumed in 2012 for NYC is 54 TWh [35]. Buildings in NYC account for two-thirds of the total annual electricity consumption [36]. Thus, out of the 54 TWh, building energy consumption alone accounts for approximately 36 TWh. Based on our model simulation, the annual electricity consumption for 2012 is 34 TWh, which is remarkably close and differs from the actual electricity consumption by a mere 5%. As noted before, the building classification used from the PLUTO database does not account for 9% of the buildings in NYC (Hospitals, Warehouse, etc.). The exercise has shown that the single building energy model can be scaled to represent neighborhood and even city scale consumption with the help of a detailed building dataset and a suitable building classification scheme.

3.2. Coupled Simulation:

292
293
294
295
296
297
298
299
300
301
302
303
304
305
306
307
308
309

From the two-way simulations of the WRF model coupled with the building energy model, we studied the relationship between building energy use and its impact on the surrounding environment during a 10-day period in July 2012. Fig. 4a shows the average peak hour (1200 - 1700 local time) air conditioning demand for the New York Metropolitan area (the encapsulated space shows the innermost domain of the simulation of 1 km resolution). Similar to the SBEM, the WRF simulation also shows high energy consumption in most of Manhattan, dominated by tall structures and commercial buildings. A distinct gradient can be deduced as we move away from the center of the City. The neighborhoods in Brooklyn and Queens, dominated by 2-story residential houses have much lower energy footprint. The energy demand fades from 26-27 Wm⁻² in Midtown Manhattan to 10-12 Wm⁻² in Brooklyn and Queens. The gradient reduces to 3-4 Wm⁻² as we move further North East to Long Island which is mostly a suburban neighborhood with high vegetative fraction. The area to the west of the City in New Jersey is a highly industrialized zone and also includes Jersey City and Hoboken. The air-conditioning demand in the region averages around 12-14 Wm⁻², equivalent to Brooklyn and Queens. Overall the peak hour AC demand for Manhattan averages around 1.36 GW for the entire City

310
311
312

Fig. 4b shows the fraction of energy contributed by waste heat release from the air conditioning unit to the overall available energy. The available energy can be interpreted from the urban surface energy budget as defined below;

313
314
315

$$R_n - \Delta G = H + LE + Q_A \quad (1)$$

316
317
318
319
320

In the above Eq., R_n represents net radiation and the ΔG represents storage heat flux. H and LE are the surface energy fluxes and Q_A represents the anthropogenic heat. The left-hand or the right-hand side of the Eq. 1 is collectively referred to as the available energy. The fractional contribution was the calculated using the following Eq.;

321

$$\frac{Q_A}{R_n - \Delta G} \quad (2)$$

322 It should be noted that the anthropogenic heat in Eqs. 1 and 2 is only from the air conditioning
323 system. Heat from transportation and other anthropogenic sources are not included as the current
324 modeling framework does not account them. In NYC heat released from transportation could be
325 high due to the substantial underground rail network that connects the entire City.
326

327 It is evident from Fig. 4 that nearly 18% of the available energy in the city center (Manhattan) is
328 directly due to heat released from the HVAC system. The fractional contribution decreases
329 marginally in the outer Boroughs, dropping to 8-11 %. As we move away from the City, the
330 contribution reduces to less than 2%. The numbers indicate considerable heat added in to the
331 urban boundary layer from air conditioning use. The heat released from the air conditioning
332 system is transported within the Urban Boundary Layer (UBL) as sensible heat, which highly
333 influences the near surface air temperature and any increase in sensible heat will directly lead to
334 increase in air temperature, which will reduce the efficiency of the HVAC system, thereby
335 creating a negative feedback loop. It should be noted that the air temperature is also affected by
336 various other parameters like the turbulence structure of the urban boundary layer, humidity in
337 the lower atmosphere and other geophysical factors.
338

339 As discussed above, the building energy demand is highly dependent on the meteorological and
340 thermodynamic state of the urban environment. The panel plots in Fig. 5 compare building
341 energy use and air temperature during an average summer day and a heatwave day; the barbs
342 indicate wind direction and wind speed at 10 m. Here July 13, 1700 local time and July 18, 1700
343 local time are chosen to represent normal and heatwave conditions. Heatwaves are mesoscale
344 events caused by continental scale blocking and regional scale imbalances in energy-water
345 budgets. The temperature contours during a regular day show a high of around 31°C in much of
346 Manhattan and the temperature gradually decreases as we move towards the coast; the
347 temperature reduces to 27-26 °C in neighborhoods surrounding the coast. The wind barbs show
348 presence of a strong sea breeze during the normal day (Fig 5a). The coastal winds penetrate
349 through much of NYC, reaching far in to New Jersey. As we move east, in NYC the air
350 temperature gradient strictly follows the urban parcels proximity to the coast. During the regular
351 day, the building energy demand in NYC has a peak value of around 22-24 Wm⁻², the
352 neighborhoods in outer boroughs and those close the coast average between 6-10 Wm⁻². This
353 observed reduction in AC demand is potentially related to both land cover characteristics as well
354 as the stronger influence of the coast. During the heatwave episode, panels b and d in Fig. 5, the
355 near surface air temperature in Manhattan averages around 36-38°C and the neighborhoods close
356 to the coast experience an average temperature of around 31°C. Most interestingly there is a
357 marked shift in wind direction, the sea breeze normally witnessed during regular days does not
358 penetrate deeper in to NYC. The Manhattan and the adjacent neighborhoods witness westerly
359 land breeze, a common phenomenon during heatwave episodes. This shift in wind direction and
360 subsidence of warm air due to high pressure blocking increases the air temperature and
361 invariably escalates building energy demand. The AC demand in the highly dense Manhattan
362 neighborhoods sharply increases to 34-35 Wm⁻². We also see increases in Queens and Brooklyn
363 Neighborhoods where the demand jumps to 12-18 Wm⁻². On average, the results show that a 5°C
364 jump in air temperature leads to 12 Wm⁻² increase in AC energy demand in Manhattan and
365 around 7 Wm⁻² increase in the outer boroughs, which represents an overall 50% - 70% jump in
366 energy demand during heatwave episodes. Overall the coupled simulations reveal a complex
367 system of heat transport in NYC. As expected high density urban parcels in Manhattan

368 experience high temperatures due to their morphological characteristics and presence of tall
369 commercial and residential buildings that overwhelmingly contribute to anthropogenic heat
370 emissions. The heat released from these parcels penetrate the neighboring parcels located in
371 Brooklyn, Queens, The Bronx and even to Upper Manhattan neighborhoods that are cut-off from
372 coastal winds during heatwave episodes.

373
374

375 **3.3. Landcover, Landuse and Building Energy Consumption**

376

377 This section explores the relationship between building energy consumption and urban land
378 cover land use. Various cities are promoting and administering measures to optimize energy
379 consumption and improve climate resiliency which primarily involves reducing urban heat island
380 effect using different green infrastructure strategies like cool roofs, urban greening, porous
381 pavements etc. Apart from the plans that focus on roofs, all other strategies are constrained by
382 space availability. Herein we analyze how building energy consumption and urban heat island
383 intensity varies in different land parcels in NYC and its relationship to the surrounding
384 landcover. The analysis is purported to identify areas within the city that will maximize the
385 benefits of green infrastructural interventions. Fig. 6 shows the relationship between annual
386 energy consumption and permeability fraction for different urban parcels. At each zip-code of
387 the City, the weighted average of permeability fraction was calculated and mapped in Fig. 7a.
388 The box plot (Fig. 6) shows a direct exponential relationship between permeability and total
389 energy use for both commercial and residential buildings. On average residential buildings
390 located in predominantly impervious parcels consume 30000 kWh compared to 1500 kWh for
391 buildings surrounded by vegetative cover. This relationship also holds for commercial buildings.
392 The relationship establishes that higher vegetative cover in a given parcel could have a direct
393 impact on energy consumption. This effect is mainly tied to the surface energy balance of a
394 given parcel. Impervious surfaces have higher heat storage capacity and overwhelmingly
395 redistribute available energy in to sensible heat as opposed to latent heat. The sensible heat will
396 directly lead to an increase in near surface air temperature which will increase the energy load of
397 HVAC systems.

398

399 Fig. 7 a, b and c show permeability fraction, annual energy use and UHI for various zip codes in
400 NYC, which indicates the administrative boundaries of the City. Apart from the mid and lower
401 Manhattan areas shown in lighter shades of green and the parks indicated in darker green shades,
402 much of NYC land parcels have a permeability fraction between 20-50%. Most of Brooklyn and
403 The Bronx area averages around 20-30% whereas Queens has an average impermeability of
404 around 50%. The difference is related to land use characteristics; Brooklyn and The Bronx
405 boroughs have many industrial parcels and Queens is dominated by residential neighborhoods.
406 Similarly, the annual energy consumption in much of Brooklyn averages around 0.2 - 0.4 GWh
407 and in Queens, most of the parcels average between 0.1 - 0.22 GWh. Most of the high-energy
408 consumption parcels are in lower Manhattan area.

409

410 The permeability index is a static variable and is solely determined by land cover characteristics.
411 The UHI and energy use indices are dependent on various meteorological factors. Here the 1-
412 week simulation data was used to calculate the UHI, which is the difference between the 2-m air
413 temperature in the urban parcels and the rural parcel. The 2-m air temperature is commonly used

414 as an indicator of ground conditions. The rural grid cells were located at 50 km north-west of
415 NYC in comparable elevation and dominated by vegetative cover. It should be noted that the
416 UHI pattern shown here is only applicable to summertime peak demand period, particularly
417 during extreme heat episodes when the energy demand is high. The UHI contours show high
418 values in much of Manhattan, including the upper Manhattan neighborhoods which have
419 relatively less heat rejection compared to lower Manhattan parcels. Also, the parcels in Queens,
420 Brooklyn and The Bronx, closer to Manhattan experience high UHI. Parcels close to the coast
421 experience relatively weaker UHI. The UHI pattern is consistent with the sea breeze pattern,
422 wherein the parcels adjacent to the coast experience weaker UHI compared to parcels in
423 Manhattan and Bronx.

424
425 Cumulatively the results show that along with commercial zones in Manhattan, the
426 neighborhoods that are adjacent to Manhattan also experience very high UHI. This is mainly
427 because of heat advection from the center of the city to downwind areas. Also during extreme
428 heat days, the sea breeze does not reach these neighborhoods. While most land parcels within
429 Manhattan have very high impervious cover, the neighborhoods adjacent to the City have
430 relatively higher fraction of pervious surfaces. In South Bronx, the permeability fraction ranges
431 between 30-50%. The parcels in Queens and Brooklyn that are closer to Manhattan have at least
432 40-50% permeability. From geophysical perspective, these neighborhoods that experience
433 disproportionately high UHI should be targeted for energy efficiency and climate moderation
434 strategies. Additionally, building level mitigation efforts such as upgrading the HVAC system
435 and increasing the reflectivity and insulation thickness of the roof and wall facets in commercial
436 districts would also potentially reduce the UHI in the surrounding neighborhoods.

437
438 Overall our results reveal that local near surface air temperature in a large urban agglomeration is
439 not a simple function of local land use and land cover characteristics. In fact, the near surface air
440 temperature in coastal NYC depends on multiple factors such as sea-breeze/land-breeze impacts
441 and proximity to heat sources.

442 443 **4. Conclusion**

444
445 Given the growing population and the increasing demand for energy in urban environments,
446 high-resolution energy models are crucial to establish the energy-environment feedbacks. In
447 order to prepare dense cities to better cope with extreme heat events, energy consumption and the
448 corresponding heat released needs to be quantified. Our study integrated coupled energy
449 modeling with high resolution land cover land use dataset to understand the spatio-temporal
450 variability in energy use pattern and its impact on the environment in the densely populated
451 NYC. The results shown here demonstrate that SBEM combined with high-resolution landcover
452 database can be used to quantify the energy use pattern at multiple spatiotemporal scales. Our
453 investigation highlighted that during extreme heat events the heat released from buildings is
454 doubled compared to regular days. To understand the environmental impacts of energy
455 consumption, the SBEM was coupled to a high-resolution urban numerical weather prediction
456 model. The simulations revealed that the heat released due to building energy consumption is 18
457 % of the total energy in the urban boundary layer. The coupled simulation study indicated that
458 during extreme heat events, areas around the high energy consuming commercial zones were
459 greatly impacted by heat advection. The residential areas downwind of the commercial zones

460 experienced disproportionately high UHI's. These regions should be the focus of urban heat
461 mitigation efforts. Furthermore, improving the HVAC efficiency of buildings located in
462 commercial zones will potentially benefit the entire city.

463

464 **Acknowledgement**

465

466 This work was supported by National Oceanic and Atmospheric Administration, Office of
467 Education Partnership Program award NA11SEC4810004, Department of Defense Army
468 Research Office, W911NF-15-1-0443.

469

470

471 **5. References**

472

473 [1] Pérez-Lombard, Luis, José Ortiz, and Christine Pout. "A Review on Buildings Energy Consumption
474 Information." *Energy and Buildings* 40.3 (2008): 394-98.

475 [2] Lewis, Aaron, and Alessandra Stuff. Inventory of New York City Greenhouse Emissions in 2014.
476 N.p.

477 [Http://www.nyc.gov/html/dem/downloads/pdf/NYC_GHG_Inventory_2014_Released_2016.pdf](http://www.nyc.gov/html/dem/downloads/pdf/NYC_GHG_Inventory_2014_Released_2016.pdf).

478 [3] Omer, Abdeen Mustafa. "Energy use and environmental impacts: A general review." *Journal of*
479 *Renewable and Sustainable Energy* 1.5 (2009): 053101.

480 [4] Conti, John, and Paul Holtberg. "Renewable Energy Outlook." *World Energy Outlook 2016* (2016):
481 397-441.

482 [5] Hillman, Tim, and Anu Ramaswami. "Greenhouse Gas Emission Footprints and Energy Use
483 Benchmarks for Eight U.S. Cities." *Environmental Science & Technology* 44.6 (2010): 1902-910.

484 [6] Zhang, Yan, et al. "China's energy consumption in the building sector: A life cycle approach."
485 *Energy and Buildings*, vol. 94, 7 Mar. 2015, pp. 240–251.

486 [7] Howard, B., L. Parshall, J. Thompson, S. Hammer, J. Dickinson, and V. Modi. "Spatial Distribution
487 of Urban Building Energy Consumption by End Use." *Energy and Buildings* 45 (2012): 141-51.

488 [8] Heiple, Shem, and David J. Sailor. "Using Building Energy Simulation and Geospatial Modeling
489 Techniques to Determine High Resolution Building Sector Energy Consumption Profiles." *Energy*
490 *and Buildings* 40.8 (2008): 1426-436.

491 [9] Oke, T.R., The energetic basis of the Urban Heat Island, Q. J. R. Meteorol. Soc. 108 (1982) 1–24.

492 [10] Ichinose, T., K. Shimodozono, K. Hanaki, Impact of anthropogenic heat on urban climate in
493 Tokyo, *Atmos. Environ.* 33 (1999) 3897–3909.

494 [11] Torrance, K.E., J.S.W. Shum, Time-varying energy consumption as a factor in urban climate,
495 *Atmos. Environ.* 10 (1975) 329–337.

496 [12] Akbari, H., M. Pomerantz, and H. Taha. "Cool surfaces and shade trees to reduce energy use and
497 improve air quality in urban areas." *Solar Energy* 70.3 (2001): 295-310.

498 [13] Caragliu, Andrea, and Chiara F. Del Bo. "Do Smart Cities Invest in Smarter Policies? Learning From
499 the Past, Planning for the Future." *Social Science Computer Review* 34.6 (2016): 657.

500 [14] Hou, Jing, Yisheng Liu, Yong Wu, Nan Zhou, and Wei Feng. "Comparative study of commercial
501 building energy-efficiency retrofit policies in four pilot cities in China." *Energy Policy* 88 (2016):
502 204-15.

503 [15] Hanna, Victor M. "Stop, Think, Build, Repeat: Using Behavioral Economics to Better Design
504 Energy Efficiency Policies for Our Cities' Buildings." *University of Miami Law Review* 69.1 (2014):
505 421

506 [16] New York NY, City of New York: one City Built to Last, 2014.

507 [17] City of Boston: Greenovate Boston 2014 Climate Action Plan Update. Boston MA, 2014.

- 508 [18] Sailor, D.J., L. Lu, A top-down methodology for developing diurnal and seasonal anthropogenic
509 heating profiles for urban areas, *Atmos. Environ.* 38 (2004) 2737–2748.
- 510 [19] Momonoki, Takashi, et al. "Evaluation of the Greenhouse Gas Reduction Effect in the Japanese
511 Residential Sector Considering the Characteristics of Regions and Households." 5 Aug. 2017
- 512 [20] Menezes, A.c., et al. "Estimating the energy consumption and power demand of small power
513 equipment in office buildings." *Energy and Buildings*, vol. 75, 2014, pp. 199–209.,
514 doi:10.1016/j.enbuild.2014.02.011.
- 515 [21] Zerroug, Abdellah , and Egils Dzelzitis. "Analysis of Results of Energy Consumption Simulation
516 with eQuest and
517 EnergyPlus." [Http://lufb.llu.lv/conference/Civil_engineering/2015/Latvia_CivilEngineering2015Vol](http://lufb.llu.lv/conference/Civil_engineering/2015/Latvia_CivilEngineering2015Vol5-102-107.pdf)
518 [5-102-107.pdf](http://lufb.llu.lv/conference/Civil_engineering/2015/Latvia_CivilEngineering2015Vol5-102-107.pdf). N.p., n.d.
- 519 [22] Ortiz, Luis E., Jorge E. Gonzalez, Estatio Gutierrez, and Mark Arend. "Forecasting Building Energy
520 Demands With a Coupled Weather-Building Energy Model in a Dense Urban Environment." *Journal*
521 *of Solar Energy Engineering* 139.1 (2016): 011002.
- 522 [23] New York City Department of City Planning, PLUTO (release 12v2), 2012 <
523 <https://www1.nyc.gov/site/planning/data-maps/open-data/dwn-pluto-mappluto.page>>
- 524 [24] New York City Department of Parks and Recreation, 2010 < <https://data.cityofnewyork.us/>>
- 525 [25] Department of Environment Protection (DEP) hydrological soil groups guideline, 2012
- 526 [26] York, Don A. "DOE-2 ENGINEERS MANUAL." [Http://doe2.com/download/doe-21e/DOE-](http://doe2.com/download/doe-21e/DOE-2EngineersManualVersion2.1A.pdf)
527 [2EngineersManualVersion2.1A.pdf](http://doe2.com/download/doe-21e/DOE-2EngineersManualVersion2.1A.pdf). N.p., Nov. 1982.
- 528 [27] Skamarock, W. C., and Coauthors. *A Description of the Advanced Research WRF Version 3*. NCAR
529 Technical Note NCAR/TN-475+STR, doi:10.5065/D68S4MVH. 2008
- 530 [28] Mlawer, Eli J., Steven J. Taubman, Patrick D. Brown, Michael J. Iacono, and Shepard A. Clough.
531 "Radiative transfer for inhomogeneous atmospheres: RRTM, a validated correlated-k model for the
532 longwave." *Journal of Geophysical Research: Atmospheres* 102.D14 (1997): 16663-6682.
- 533 [29] Dudhia, Jimy. "Numerical Study of Convection Observed during the Winter Monsoon Experiment
534 Using a Mesoscale Two-Dimensional Model." *Journal of the Atmospheric Sciences* 46.20 (1989):
535 3077-107.
- 536 [30] Smagorinsky, J. "General Circulation Experiments With The Primitive Eq.s." *Monthly Weather*
537 *Review* 91.3 (1963): 99-164
- 538 [31] Mellor, George L., and Tetsuji Yamada. "A Hierarchy of Turbulence Closure Models for Planetary
539 Boundary Layers." *Journal of the Atmospheric Sciences* 31.7 (1974): 1791-806.
- 540 [32] Chen, Fei, and Ying Zhang. "On the coupling strength between the land surface and the atmosphere:
541 From viewpoint of surface exchange coefficients." *Geophysical Research Letters* 36.10 (2009)
- 542 [33] Rosenthal, Joyce Klein, Patrick L. Kinney, and Kristina B. Metzger. "Intra-urban vulnerability to
543 heat-related mortality in New York City, 1997–2006." *Health & Place* 30 (2014): 45-60.
- 544 [34] Ramamurthy, P., D. Li, and E. Bou-Zeid. "High-resolution simulation of heatwave events in New
545 York City." *Theoretical and Applied Climatology* (2015)
- 546 [35] "POWER TRENDS 2016 the changing energy landscape." *Power Trends 2016*.
547 <[http://www.nyiso.com/public/webdocs/media_room/publications_presentations/Power_Trends/Pow](http://www.nyiso.com/public/webdocs/media_room/publications_presentations/Power_Trends/Power_Trends/2016-power-trends-FINAL-070516.pdf)
548 [er_Trends/2016-power-trends-FINAL-070516.pdf](http://www.nyiso.com/public/webdocs/media_room/publications_presentations/Power_Trends/Power_Trends/2016-power-trends-FINAL-070516.pdf). N.p., 2016>
- 549 [36] Eichholtz, Piet, Nils Kok, and John M. Quigley. "Doing Well by Doing Good? Green Office
550 Buildings." *American Economic Review* 100.5 (2010).
- 551
552
553
554
555
556
557

558
559
560
561
562
563
564
565
566
567
568
569
570
571
572
573
574
575

Tables

Table 1

Distribution of buildings in NYC extracted from the PLUTO database and classified by building function. (B.)
Stands for buildings.

Building Function	# of Building in NYC	% of Building in Manhattan (43,465 B.)	% of Building in Bronx (90,008 B.)	% of Building in Brooklyn (278,127 B.)	% of Building in Queens (324,611 B.)	% of Building in Staten Island (123,530 B.)
Residential	706,880	47.91	79.06	80.48	87.31	87.15
Commercial	24,528	12.14	3.44	2.53	2.14	1.77
Mixed	48,711	23.61	4.13	7.91	3.47	1.19
Other	79,621	16.34	13.37	9.08	7.08	9.89

576
577
578
579
580
581
582
583
584
585
586
587
588
589
590
591
592
593
594
595
596

597
598
599
600
601
602
603
604
605
606
607
608
609
610
611
612
613
614
615
616
617
618

Table 2
Distribution of buildings in NYC classified by the number of floors. (B.) Stands for buildings.

Building Height Category	Range of Floors	% of Building in Manhattan (36,133 B.)	% of Building in Bronx (77,613 B.)	% of Building in Brooklyn (252,066 B.)	% of Building in Queens (290,936 B.)	% of Building in Staten Island (110,483 B.)
Low-rise	0-5	69.58	96.60	98.58	99.28	99.92
Mid-rise	6-20	27.09	3.36	1.39	0.72	0.08
High-rise	21+	3.33	0.04	0.03	0.01	0.00

619
620
621
622
623
624
625
626
627
628
629
630
631
632
633
634
635
636
637
638
639

640
641
642
643
644
645
646
647
648
649
650
651
652
653
654
655
656
657
658
659
660
661

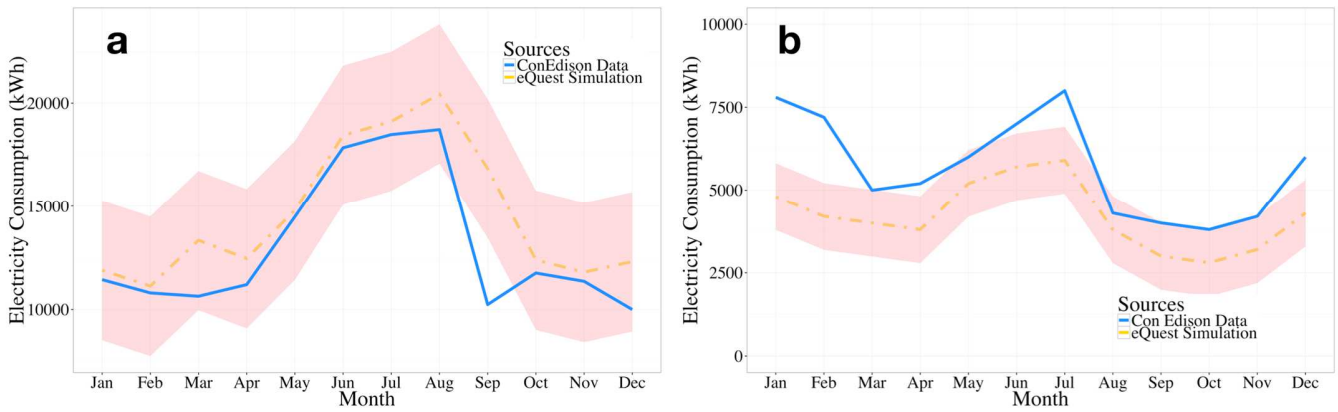
Table 3
Building properties for the SBEM used for energy consumption simulations for each building type.

Properties	Residential	Commercial	Mixed
Albedo (%)	0.6	0.6	0.6
Thermal Capacity (W/m °K)	0.519	0.346 - 0.5363	0.519
Thermal Conductivity (J/kg °K)	132.2 - 279.06	133.88 - 2467.97	133.88 - 1744.31
Wall Insulation (m ² - °K / W)	2.58	1.52	1.52
Coefficient of Performance	2.72	2.9	2.9

662
663
664
665
666
667
668
669
670
671
672
673
674
675
676
677
678
679
680
681
682
683
684

685
686
687
688
689
690
691
692
693
694
695
696
697
698
699
700
701
702
703
704

Figures



705 **Fig. 1.** Comparison of electricity consumption between energy model simulation and real data from Con Edison for
706 an entire year (a) Residential building (b) Commercial building.
707

708
709
710
711
712
713
714
715
716
717
718
719
720
721
722
723
724

725
726
727
728
729
730
731
732
733
734

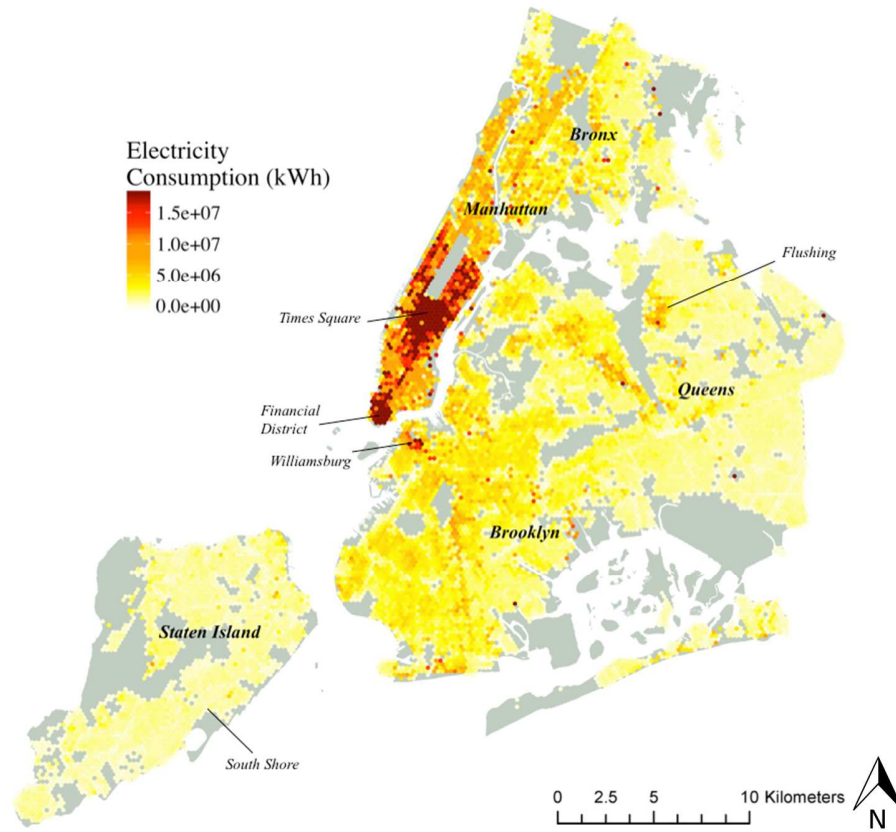


Fig. 2. Spatial distribution of the electricity consumed in NYC for one year.

735
736
737
738
739
740
741
742
743
744
745
746
747
748
749
750
751

752
753
754
755
756
757

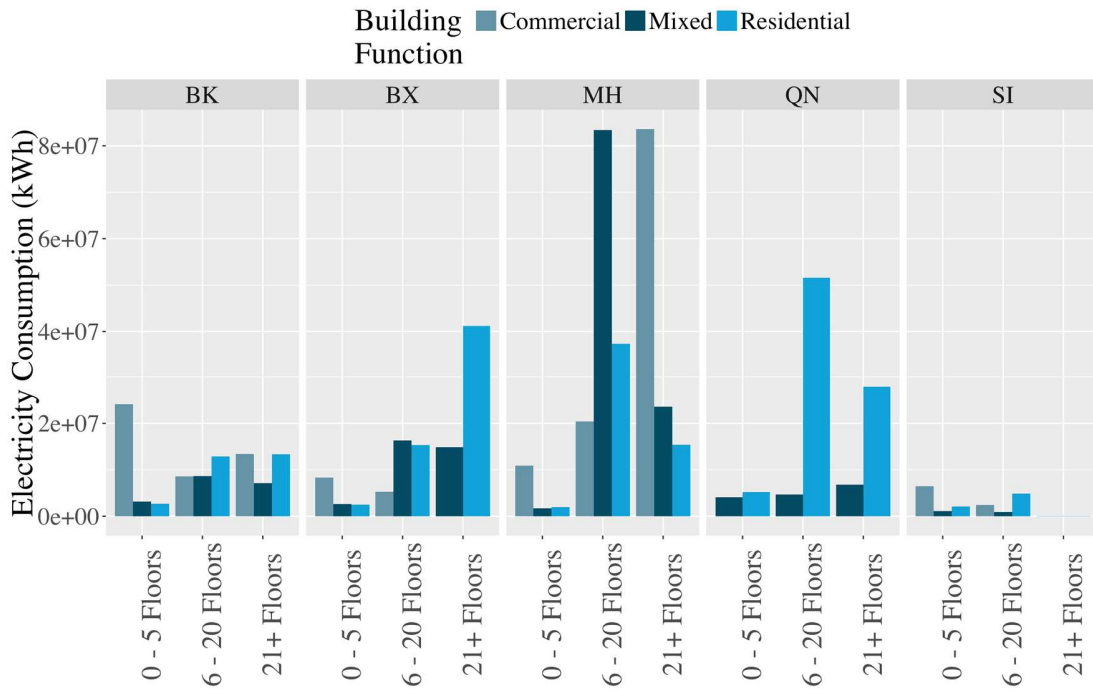
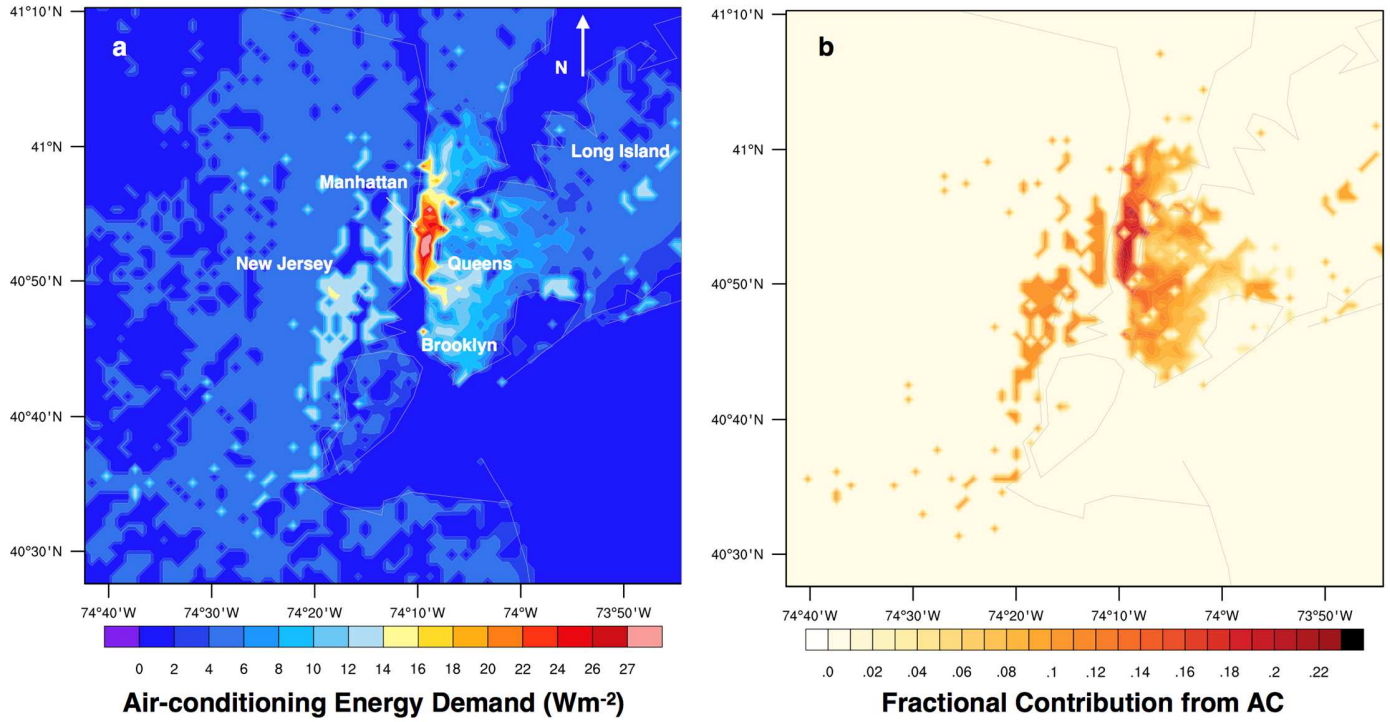


Fig. 3. Total annual electricity consumption for each building function and category.

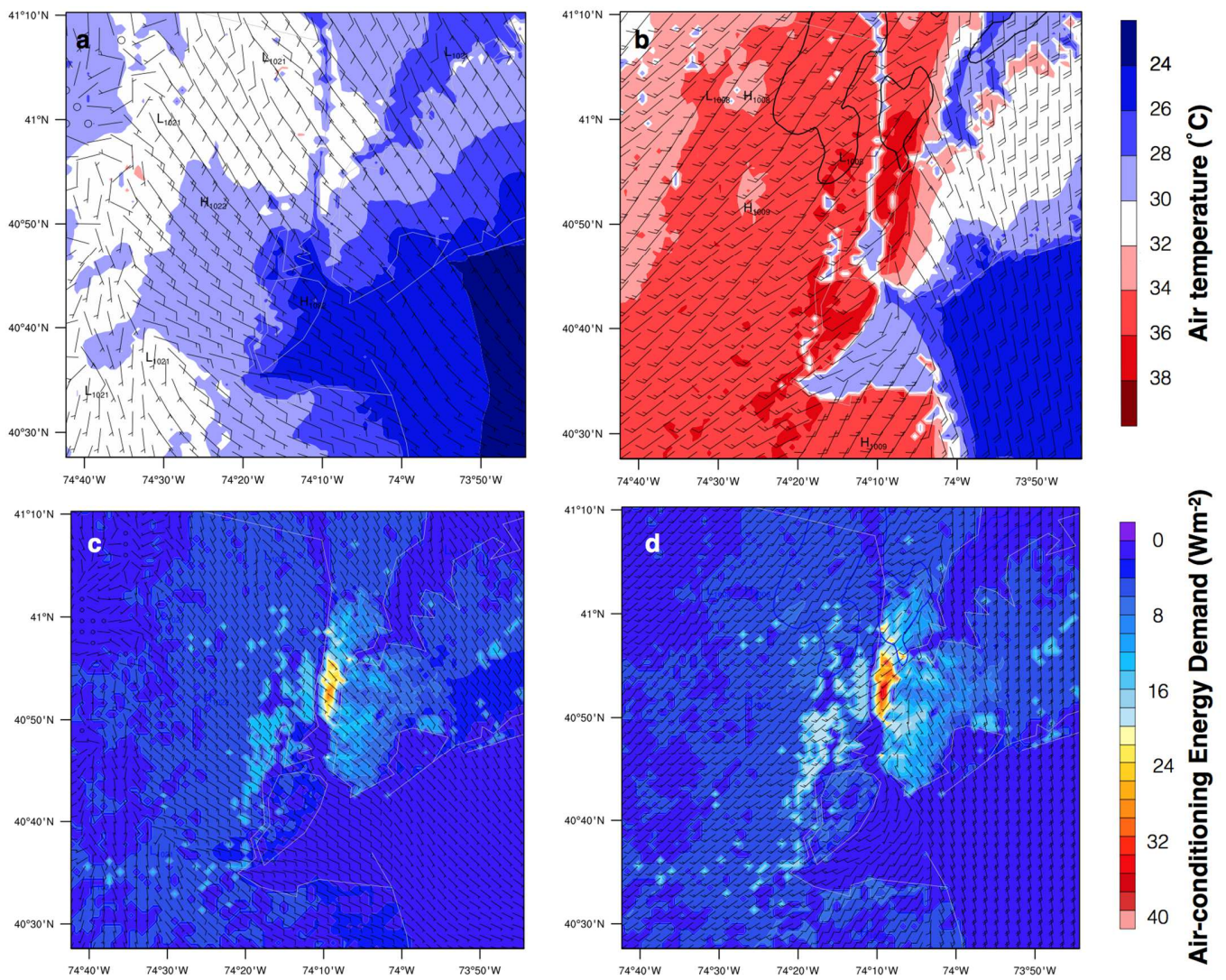
758
759
760
761
762
763
764
765
766
767
768
769
770
771
772
773
774
775
776
777
778
779
780
781
782
783

784
785
786
787
788
789



790
791
792
793
794
795
796
797
798
799
800
801
802
803
804
805
806
807
808

Fig. 4. (a) Average air conditioning demand for New York City (b) Fraction of energy contributed by waste heat release from the air conditioning unit to the overall available energy.



810 **Fig. 5.** (a) Air temperature during an average summer day (b) Air temperature during a heatwave day (c) Building
 811 energy use during an average summer day (d) Building energy use during a heatwave day
 812
 813
 814
 815
 816
 817
 818
 819
 820
 821
 822
 823
 824
 825
 826

827
828
829
830
831
832
833
834
835
836
837
838
839
840

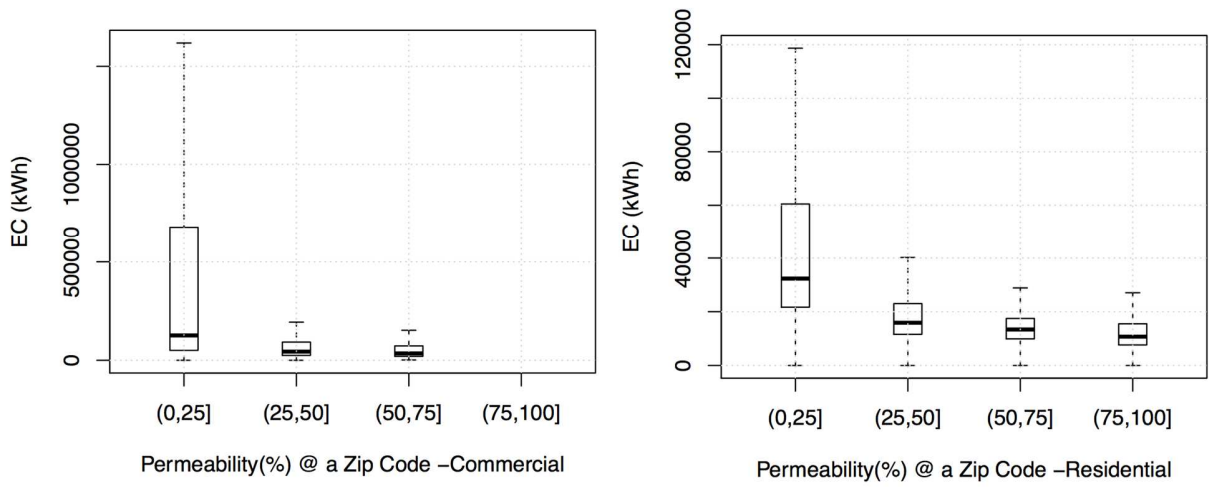
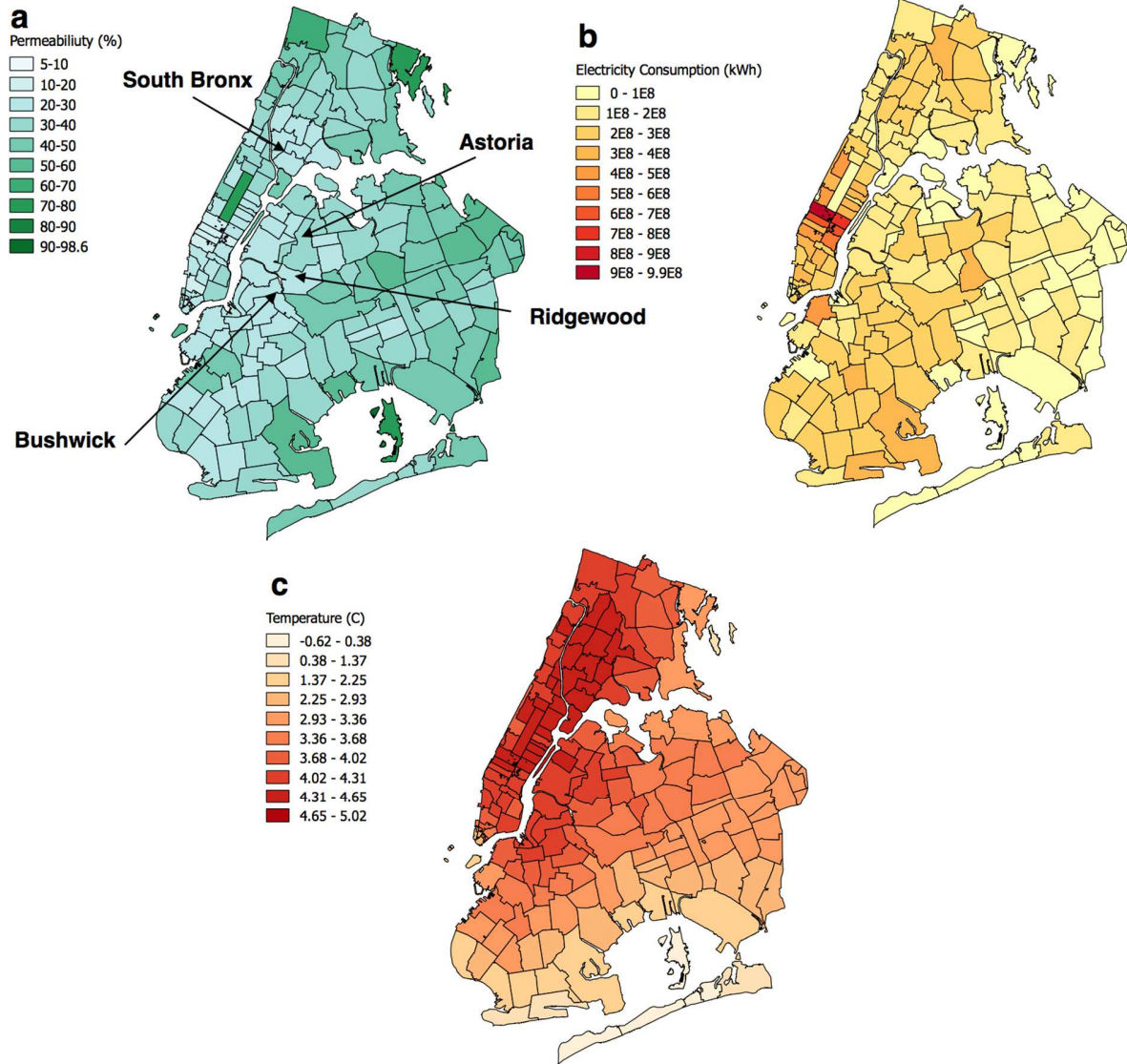


Fig. 6. Annual energy consumption and permeability fraction for commercial and residential buildings.

841
842
843
844
845
846
847
848
849
850
851
852
853
854
855
856
857
858
859
860
861
862
863
864
865
866

867



868

869
870

Fig. 7. Permeability coefficient, annual energy use and UHI for various zip codes in NYC.

871
872
873
874
875
876
877